Role of the Oxyallyl Substructure in the Near Infrared (NIR) Absorption in Symmetrical Dye Derivatives: A Computational Study

Ch. Prabhakar, G. Krishna Chaitanya, Sanyasi Sitha, K. Bhanuprakash,* and V. Jayathirtha Rao*,†

Inorganic Chemistry Division and Organic Chemistry Division, Indian Institute of Chemical Technology, Hyderabad-500 007 India

It is well-known from experimental studies that the oxyallyl-substructure-based squarylium and croconium dyes absorb in the NIR region of the spectrum. Recently, another dye has been reported (*J. Am. Chem. Soc.* **2003**, *125*, 348) which contains the same basic chromophore, but the absorption is red-shifted by at least 300 nm compared to the former dyes and is observed near 1100 nm. To analyze the reasons behind the large red shift, in this work we have carried out symmetry-adapted cluster−configuration interaction (SAC−CI) studies on some of these NIR dyes which contain the oxyallyl substructure. From this study, contrary to the earlier reports, it is seen that the donor groups do not seem to play a major role in the red-shift of the absorption. On the other hand, on the basis of the results of the high-level calculations carried out here and using qualitative molecular orbital theory, it is observed that the orbital interactions play a key role in the red shift. Finally, design principles for the oxyallyl-substructure-based NIR dyes are suggested.

Introduction

Functional dyes are of current research interest, because they find applications in optical devices such as optical switches and saturable absorptive mirrors, and as materials in electrophotographic reproduction, solar cells, and so on.[1−4] Of particular interest are the organic functional dyes, because these have features such as flexibility and high interaction with light, and over and above all these is the custom-tailored synthesis of the dye in the absorption range of our choice. Here, computational chemistry based on quantum chemical theories, which are replacing the earlier empirical rules, is playing a major role in understanding the dyes post priori experiment or in suggesting modifications, a priori synthesis, suitable to the applications.[1−2] Recent studies of organic dyes have concentrated in the absorption range greater than 1000 nm, as these are useful in telecommunications, medicine, semiconductor lasers, and so forth.[5−7] Because these absorb in the near-infrared region, these dyes are also referred to as NIR dyes.[1] Basically, to absorb in the NIR region, the HOMO−LUMO gap has to be small, and this in principle can be obtained through extended π-conjugation or introducing heavy elements into the backbone. But the drawback is that these are labile.[8] Hence, absorption in the NIR region with a smaller chromophore poses a challenge.

Some promising NIR dyes with small chromophores are the squaric acid derivatives (Figure 1a), croconic acid derivatives (Figure 1b), and very recently synthesized derivatives of di-(benzofuranonyl)methanolate (BM) (Figure 1c), all of which contain the oxyallyl substructure (Figure 1d).[5] While the squaric acid derivatives absorb at slightly lower wavelengths (600−800 nm) when compared to the croconic acid derivatives (700−900 nm), the BM derivative absorbs around 1100 nm, a much longer wavelength (around 300-nm bathochromic shift) than the

former ones.[1−2] This red shift is astounding, given that the chromophore is small. Langhals analyzed the reason for this drastic red shift.[8] It was suggested that the carbenium ion is the acceptor, and on the basis of the empirical model of Konig and Ismailsky of D−π−A−π−D (D = donor and A = acceptor),[9−15] absorbance in the longer-wavelength region is due to the increased π-conjugation. When this acceptor is replaced by squaric acid, which contains two formal positive charges, the absorption shifts to the red. And on further replacement of the squaric acid by croconic acid, which is supposed to contain three positive charges, a larger red shift is seen. In addition, the large bathochromic shift of the BM derivative has been reasoned out to be due to the two carbonyl groups of the lactone rings which act as super acceptor groups to the mesoionic structure, and the amino groups act as donors. On the basis of this model, it was suggested that the donor groups if replaced by super donor groups should also result in larger bathochromic effects.[8] Tatsuura et al. suggested that there are two main reasons for this bathochromic shift: one which arises because of the concentration of π-electrons in the center region of the molecule and the lactone groups acting as the super acceptors and the other due to the twisting of the benzofuranonyl groups.[6]

An important question from the design point of view remains to be answered: Can we get a larger red shift by increasing the donation capacity of the donor groups? In other words, are these type of molecules really D−A−D? To understand the mechanism of the absorption, it would be ideal to first understand the charge transfer in the related dyes, namely, the squaric acid and croconic acid derivatives. Not many of such studies have been reported.[16−19] In the case of the squaric acid derivatives, Bigelow and Freund reported modified neglect of differential overlap (MNDO) and complete neglect of differential overlap/spectroscopic CNDO/S (single + double energy selected configuration interaction) calculations and arrived at the conclusions that the singlet−singlet transition (S0−S1) has large oscillator strength because of the HOMO−LUMO orbital delocalization over the

   * E-mail: bhanu2505@yahoo.co.in (IICT communication no. 050102/ CMM0022).
   † Organic Chemistry Division.

Oxyallyl-Substructure-Based NIR Dyes

J. Phys. Chem. A, Vol. 109, No. 11, 2005 **2615**

(a) Squarylium Dye

(b) Croconium Based Dye

(c) BM Dye Derivative
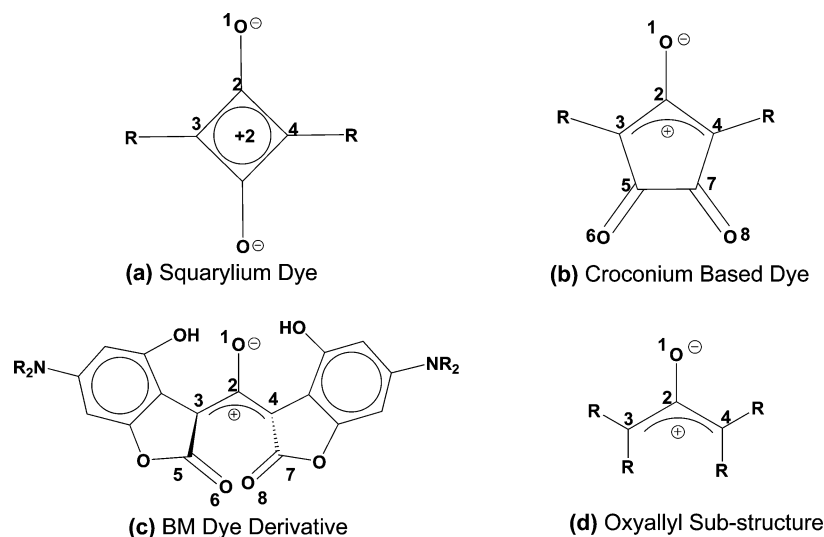
(d) Oxyallyl Sub-structure

Figure 1. Molecular structures of the dyes: (a) squarylium dye, (b) croconium-based dye, (c) BM dye derivative, and (d) oxyallyl substructure.

backbone, and the amino group nitrogen donates very little charge. On the other hand, the oxygen atoms act as acceptors in the ground state and as donors in the excited state, which inhibits the charge transfer.[16] The major conclusion is that these are $\pi-\pi^*$ transitions occurring at the center of the molecule (i.e., the squaraine moiety). Studies by Law on the molecular structure changes leading to absorption changes in squaraine dye derivatives showed that there is very little shift of the absorption band on substitution and changing of solvents.[20] This has been attributed to the noninvolvement of the donor group in the S_0-S_1 excitation. Meier et al. recently studied experimentally the effect of increasing the conjugation using stilbenoid moieties on the squaraines (3,4-substituted in Figure 1). They observed that there was first a bathochromic shift of ∼300 nm and a further increase of conjugation brings in a hypsochromic shift of ∼200 nm, in contrast to the normal conjugated oligomers which show a convergence of the absorption.[21] They conclude that this influence of the stilbene-building moieties on absorption is not in line with the quantum chemical treatment of the squaraines carried out by Bigelow and Freund, where it was suggested that the entire charge localizes on the central ring.[16] In the case of croconic acid derivatives, the 3,4-amino derivative (in Figure 1) shows a singlet–singlet excitation energy which is very large (around 440 nm), and it has been attributed to distortion of the molecule.[1,22] But by increasing the conjugation and twisting the aminobenzyl group, the absorption is around 860 nm.[5] After replacing the end groups with heterocyclic rings, the absorption of the molecule is still around 830 nm.[1,23]

In light of these observations on dyes and also the importance of the design principles in functional dyes, we have undertaken the study of the role of this substructure in the singlet–singlet absorption of dyes which contain this unit, using high-level calculations, namely, the SAC–CI method.[24−28] Our main aim would be to see how the same substructure in different types of dyes shows absorptions of so much variation and if we could suggest modifications which would enhance the bathochromic shift in this small π-system.
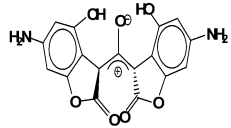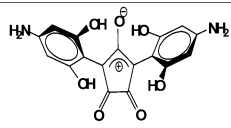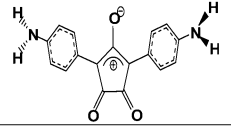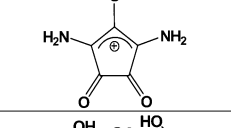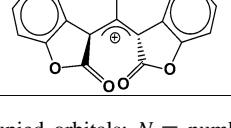
Computational Details

Earlier theoretical studies of the molecules containing the oxyallyl substructure have been carried out by Gleiter and Hoffman.[29] They reveal that the singlet structure is stabilized relative to the triplet and is the ground state when the conjugation in the molecule is increased or when withdrawing

groups are substituted. Calculations carried out by Hrovat et al. indicate that even in the simple oxyallyl substructure (which is considered to be in resonance between the zwitterionic and diradicaloid forms) the zwitterionic resonance form (Figure 1d) makes a modest contribution and the ground state is a singlet, $^1A_1$.[30] Larger conjugated groups and/or heteroatoms as substitutions stabilize the zwitterionic character and enhance its contribution to the ground state.[2] Experimental evidence of this is based on the intense absorption bands of these dyes that suggest extensive delocalization of the charge on the backbone of the molecule.[20] Hence, we concentrate on the ground-to-singlet-state transitions of these dyes in this work. We chose five molecules for our study, which are shown in Table 1. The first molecule is the BM derivative, and the second one is the croconic acid derivative in which the oxyallyl substructure, along with the ring, is planar, unlike the former molecule. Our aim here is to compare these two molecules and understand why molecule **1** has such a large red shift. Molecule **5** has been chosen to understand the role of the amino groups in molecule **1**. Molecules **3** and **4** have been chosen to study the effect of conjugation and substitution in this substructure.

It is well-known that, for diradicaloid derivatives, double excited configurations, in addition to single excited configurations, are also of importance for the description of the singlet ground state and its transitions.[31] Evidently, this is because of the smaller energy differences between the orbitals, which give rise to more contributing determinants to the state energy. Hence, the singles CI based on Zerner's intermediate neglect of differential overlap (ZINDO) and ab initio/CIS are not found suitable.[32−33] In fact, our initial calculations using these methods show that the results deviate from the experimentally determined values by 300−500 nm, and hence, they are not reported here. On the other hand, SAC/SAC−CI methods which take into consideration the singly and doubly excited states have been found reliable for studying molecular spectroscopy.[24−28] The detailed methodology of this is given elsewhere, but we give the salient features of our calculations here.[28]

The geometries of the molecules have been optimized by the B3LYP/6-31G(d,p) method using the ab initio software *Gaussian 03W*, and for comparison, the HF/6-31G(d,p) method is also used for optimization of the geometries.[34] The geometries so obtained using these two methods have then been subjected to the SAC/SAC−CI calculations using *Gaussian 03W*.[35] For the ground state, SAC is carried out and is nonvariational, while

TABLE 1: Details of the SAC/SAC−CI Calculations Carried Out Using the B3LYP/ 6-31G(d,p) Optimized Geometries

Mol. No.	Structure	Sym	Active Space $(M, N)^a$	SAC		SAC-CI	
				No. of Configurations ^{b}	Linked operators ^{c}	No. of Configurations ^{b}	Linked operators ^{c}
1		C_2	(41, 120)	10	6056520/ 28755	19	6054060/ 101826
2		C_2	(41, 120)	15	6056526/ 25071	17	6054054/ 121638
3		C_2	(41, 130)	11	7107555/ 45487	14	7104890/ 114663
4		C_{2v}	(26, 134)	4	1602652/ 58114	19	1600638/ 83863
5		C_2	(41, 110)	13	5089541/ 31209	17	5087274/ 123290

^{a} M = number of occupied orbitals; N = number of virtual orbitals. ^{b} Number of configurations that have CI coefficients larger than 0.03. ^{c} Linked operators total generated/selected.

TABLE 2: Optimized Geometrical Parameters and Dipole Moments (in debye) of the Structures Calculated in This Work Using the B3LYP/6-31G(d,p) and HF/6-31G(d,p)^a Methods

molecule no	C2−O1 (Å)	C2−C3 (Å)	C−N (Å)	C5−O6 (Å)	bond angles (°)		dipole moment^b
					O1−C2−C3	C3−C2−C4	
1	1.305	1.424	1.364	1.199	119.3	121.3	2.37
	(1.294)	(1.404)	(1.347)	(1.173)	(119.6)	(120.8)	(1.52)
2	1.268	1.463	1.360	1.235	123.7	112.6	4.72
	(1.247)	(1.442)	(1.345)	(1.198)	(124.2)	(111.6)	(3.85)
3	1.244	1.470	1.365	1.227	126.0	107.9	6.14
	(1.224)	(1.451)	(1.357)	(1.195)	(126.1)	(107.9)	(5.35)
4	1.240	1.448	1.321	1.225	128.3	103.4	3.53
	(1.221)	(1.429)	(1.310)	(1.194)	(128.1)	(103.8)	(2.79)
5	1.301	1.425		1.199	119.6	120.7	2.25
	(1.287)	(1.405)		(1.173)	(120.1)	(119.9)	(1.49)

^{a} Values obtained using the HF-6-31G(d,p) optimized geometries are in parentheses. Only the substructure's geometrical parameters in each molecule are reported. Atom numbers are shown in Figure 1. ^{b} Dipole moment lies along the z-axis.

for the excited state, SAC−CI is carried out using the variational methods.[28] The active space is chosen with the window option where, depending on the molecule's size, some core and some virtual molecular orbitals (MOs) are not used in the active space. In most of the cases, the active space is always found to have at least 160 orbitals for the excitations. To the ground state, all the single excitation operators in this are included without selection. For the doubles excitation operators, an energy threshold value of 5.0×10^{-6} hartree is used to select the configurations based on a perturbation method. The details of the SAC and SAC−CI carried out here are given in Table 1. Unless mentioned otherwise, the discussions in this work will be based on B3LYP/6-31G(d,p) optimized geometry.

The SAC−CI is also restricted to singles and doubles linked operators, while the higher-order ones are treated through unlinked operators. For each molecule, four lowest excited states are requested. The double excitation operator selection of the configurations is again based on a perturbation approach. Here, the interaction with the reference states is carried out, and any configuration that has an interaction energy greater than the threshold value of 5.0×10^{-7} hartree is selected. Raising the threshold to 1.0×10^{-5} hartree for the SAC and 1.0×10^{-6} hartree for the SAC−CI brings about a change in the absorption energy of a maximum of 0.1 eV in one or two cases; hence, the convergence is nearly achieved. The molecular orbital plots have been generated using MOPLOT.[36]

Results and Discussion

A. Geometry, Charge Density, and Dipoles. Optimized geometries obtained using both HF/6-31G(d,p) and B3LYP/6-31G(d,p) methods are shown in Table 2. As we are interested in the geometry changes due to substitution in the oxyallyl substructure, we report only the bond lengths and bond angles of the substructure in the table. It is observed that the HF-based bond lengths are slightly smaller than the B3LYP geometries. This is because B3LYP is a correlated method and to a certain extent mixes the charge-separated and the diradicaloid states.

Oxyallyl-Substructure-Based NIR Dyes

J. Phys. Chem. A, Vol. 109, No. 11, 2005 **2617**

So, minor changes in the geometry are to be expected between these two. In the case of molecule **1**, both methods predict a lengthened CO bond, indicating the single bond character. Both the CC bonds inside the moiety are predicted to be double bonds, and this has a value of 1.424 Å, obtained using the density functional theory (DFT) method. The CO bond is slightly smaller in **2**, which is a croconic acid derivative, compared to **1**. On the other hand, the CC bond length is slightly elongated. In both cases, the lengthened bond should create a negative charge on the oxygen atom, which is stabilized by the hydrogen bonds of the hydroxyl groups. Thus, a charge-separated kind of structure is dominant in the ground state, and further evidence at the SCF level is seen from the dipole moments shown in the same table. By comparing the dipole moments of molecules **1** and **2**, it is seen that the latter has a larger dipole moment. This indicates that in **2** the charge stabilization in the molecule is larger. Molecule **3** is a planar molecule, and the entire molecule is in conjugation, unlike in **2** where the side groups have been rotated. The conjugation further stabilizes the positive charge on the backbone, and this is also evident from the much larger dipole moments. The CO bond length is now reduced to 1.244 Å and in fact remains nearly at the same length in **4**, which is a croconic acid derivative disubstituted by amino groups. The CC bond lengths are much longer in the latter molecules, **3** and **4**, than in **1**. The CCC bond angles vary from 121.3° in molecule **1** to 103.4° in **4**. Further stabilization in all the molecules is due to the carbonyl groups in the 5 and 7 positions, which have a slightly elongated CO bond when compared to the standard carbonyl groups. An NR_2 group substituted to the side aromatic rings also stabilizes the charge through the mesomeric effect. This is evident from the shortening of the CN bonds shown in the same table. On the basis of these discussions, it is clear that the oxyallyl substructure in all the molecules can be represented by the charge-separated moiety, and in the planar molecules, the separation is much more stabilized. Dipole moments aligned on the symmetry axis, as is expected, pass through the central CO bond in all the molecules.

B. SAC/SAC−CI Study. The symmetric HF ground state ($^1A/^1A_1$) of all the molecules is improved by SAC, and the configurations contributing to this state are shown in Table 3. To the ground state in SAC studies, the HF contribution will be 1.00, and this is indicated in the table. Small but reasonable contributions (mixing coefficients of >0.05) from the excited states are shown in the table. We shall concentrate on the important excited-state contributions in **1** and **2**, to bring out the difference between the two. The MOs of the two molecules are compared in Figure 2. They are observed to be nearly the same. Thus, in the case of **1**, the major contribution comes from the double excited configuration (HOMO−LUMO), which has a fairly large contribution of 0.09. This orbital excitation decreases the charge density in the center part of the molecule and inducts a diradicaloid type of structure into the ground state. The next two double excitations, which have a mixing coefficient of about 0.06, are basically the excitations in the phenyl rings, and there is no movement of charge at the center. Another important configuration (not shown in the table) is the HOMO-3 to the LUMO double excitation, and this has a contribution of 0.036 but involves a small charge transfer from the amino groups to the central part. Two other configurations, one the singly excited HOMO−LUMO + 1 (CI coefficient of 0.031) and the other the double excitation HOMO−LUMO + 1 (−0.038) also involve charge transfer to the carbonyl groups in the ground state in addition to the previously mentioned ones. The situation in **2** for the SAC ground state is no different. Here, there is no

TABLE 3: Main Configurations and Mixing Coefficients for the Singlet Ground and Excited States Obtained with SAC/SAC−CI Method Using the B3LYP/ 6-31G(d,p) Optimized Geometries

molecule	state	mixing coefficient[a]	configuration
1	^1A	1.000	$91b^2, 92a^0$
		−0.090	91b−92a, 91b−92a
		0.060	90b−94b, 89a−95a
		0.058	90b−95a, 89a−94b
	^1B	0.934	91b−92a
		0.082	87b−92a
		−0.180	91b−93b, 91b−92a
		−0.105	91b−92a, 88a−92a
		−0.094	91b−93b, 87b−92a
		0.090	88a−92a, 87b−92a
		−0.078	91b−105b, 91b−92a
2	^1A	1.000	$92b^2, 93a^0$
		−0.086	92b−93a, 92b−93a
		0.066	91a−98a, 90b−97b
		0.065	91a−97b, 90b−98a
		0.050	92b−94b, 88b−94b
	^1B	0.935	92b−93a
		0.076	89a−95b
		0.200	92b−93a, 89a−93a
		−0.096	92b−93a, 87a−93a
		0.082	92b−93a, 85a−93a
3	^1A	1.000	$76b^2, 77a^0$
		−0.067	76b−77a, 76b−77a
		−0.056	74b−81b, 73a−80a
		−0.053	74b−80a, 73a−81b
	^1B	−0.951	76b−77a
		−0.133	76b−77a, 75a−77a
		0.093	75a−77a, 72b−77a
		−0.080	76b−79b, 76b−77a
4	$^1A_1$	1.000	$36b_1^2, 37a_2^0$
		−0.060	$36b_1−37a_2, 36b_1−37a_2$
	$^1B_2$	0.935	$36b_1−37a_2$
		0.138	$33b_1−37a_2$
		0.084	$26b_1−37a_2$
		−0.185	$36b_1−43b_1, 36b_1−37a_2$
		0.097	$36b_1−44a_2, 36b_1−38b_1$
		0.083	$36b_1−38b_1, 30b_1−37a_2$
		0.076	$36b_1−38b_1, 36b_1−37a_2$
5	^1A	1.000	$83b^2, 84a^0$
		−0.091	83b−84a, 83b−84a
		0.050	82a−88a, 81b−87b
		0.050	82a−87b, 81b−88a
	^1B	−0.925	83b−84a
		−0.119	79b−84a
		−0.100	81b−84a
		−0.087	67b−84a
		0.181	83b−85b, 83b−84a
		0.089	83b−84a, 82a−84a
		−0.086	80a−84a, 79b−84a
		0.077	83b−93b, 83b−84a
		0.071	83b−84a, 80a−84a

[a] CI coefficients of the ground state are larger than 0.05. CI coefficients of the excited state are larger than 0.07. For the SAC, by definition, the coefficient of HF configuration is always 1.00.

single excitation with a CI coefficient larger than 0.03, but small contributions are seen in the double excitations. The doubly excited HOMO−LUMO has a contribution of 0.086, which is slightly smaller than the previous case. The amino group donation to the central part is seen in HOMO-3 to LUMO double excitation with a contribution of 0.038. There is a larger charge transfer from the phenyl groups to the carbonyl groups, which is seen as HOMO−LUMO + 1 and HOMO-4−LUMO + 1 excitation.

The major contributions to the excited state ($^1B/^1B_1$) are obtained by SAC−CI, and these are shown in the same table. In all the molecules, the major contribution is from the HOMO−LUMO single excitations, which contribute almost 93%. Small
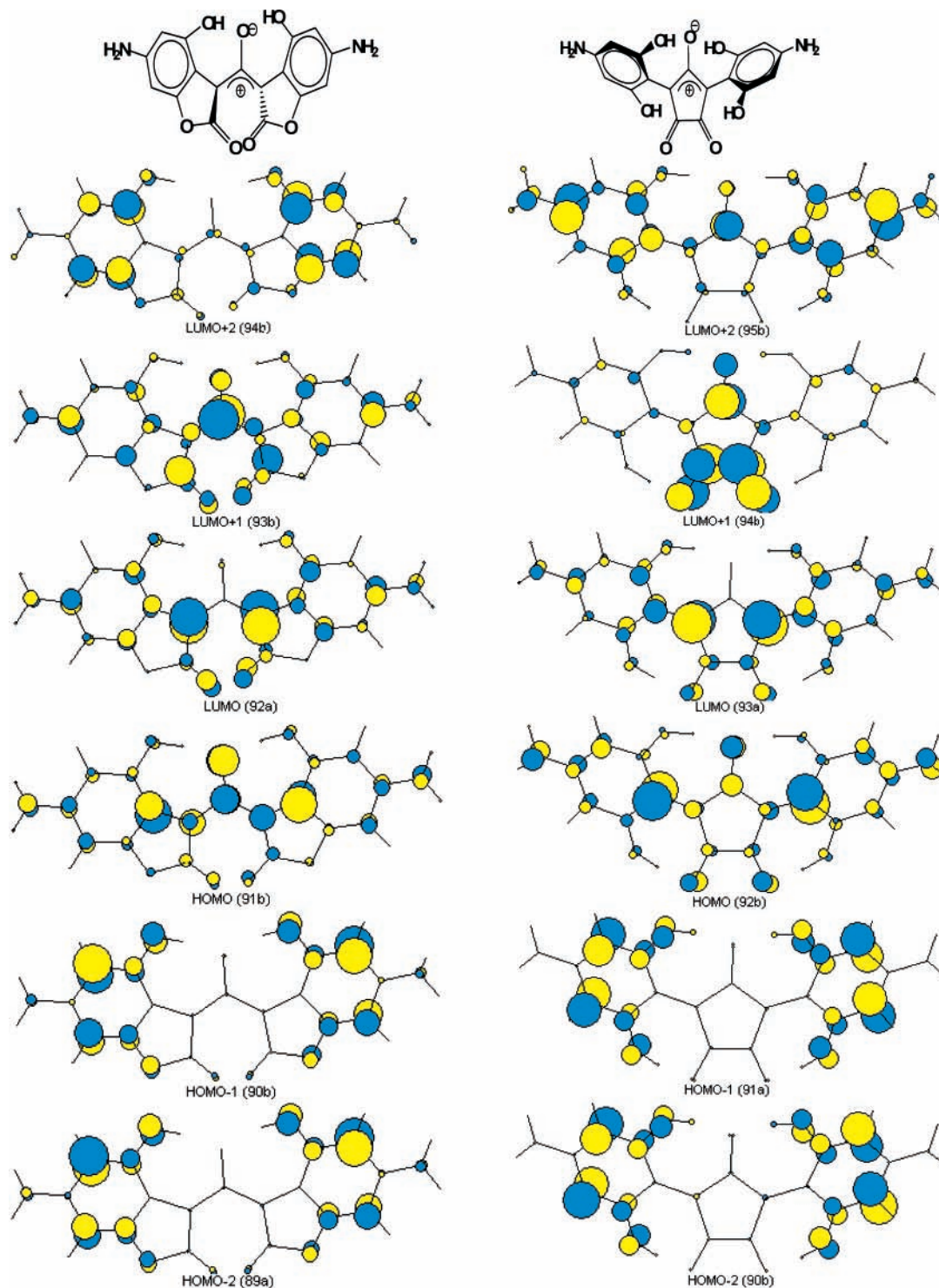
Figure 2. Comparison of the MOs of molecules **1** and **2**. The orbital symmetry and orbital numbers are given in parentheses.

but reasonable contributions to this state from the excited states are also seen. In contrast to the ground state and as expected, more singly excited states contribute this state. But again, there is no major difference between **1** and **2**. In both cases, the contribution of the orbital excitation in which there is a small charge transfer from the donor amino groups to the center has a CI coefficient of 0.07−0.08. This also involves charge transfer from the oxygen atom to the central ring and so is also seen in another single excitation where the CI coefficient is around 0.06 in both molecules. In the case of double excitations, the CI coefficient has a greater contribution and has a value of >0.1 in a couple of cases. Here, the orbital excitations in which the

charge from the oxygen of the central ring (HOMO) flows to the allylic part has a larger contribution of 0.18 (in **1**) and 0.2 (in **2**). Small charge transfers from the amino groups to the central moiety in the doubly excited states as seen in HOMO− LUMO and HOMO-3−LUMO excitation in **1** and HOMO-3 −LUMO and HOMO-4−LUMO in **2**. The inference of these observations is that some charge transfer from the oxygen atom and the amino groups to the central part does take place, and also, some small charge transfer is observed in **1** to the carbonyl groups. The other small difference observed is a small contribution of the excitations in which charge transfer to the carbonyl groups takes place in the ground state in **2** but is not prominent

Oxyallyl-Substructure-Based NIR Dyes

J. Phys. Chem. A, Vol. 109, No. 11, 2005 **2619**

TABLE 4: Charge Densities in the Substructure Using SAC Obtained for the B3LYP/6-31G(d,p) Optimized Geometries[a]

molecule	O1	C2	C3	C5	O6	N
1	−0.89	0.50	−0.12	0.82	−0.49	−0.76
2	−0.82	0.48	−0.07	0.46	−0.60	−0.76
3	−0.67	0.51	−0.13	0.45	−0.54	−0.76
4	−0.63	0.46	0.20	0.42	−0.53	−0.72
5	−0.87	0.50	−0.11	0.82	−0.48	

[a] Atom number is shown in Figure 1.

in **1**. SAC of the other molecules, **3** and **4**, also show small contributions of the amino group charge transfer in the ground state while the dominant configuration is that of HF. A small contribution from the carbonyl groups to the central part is also seen in the excited state of **4**. Molecule **5** is similar to **1**.

Mulliken population analysis obtained at the SAC level for the ground state is shown in Table 4. There is still substantial charge separation, which is indicated by large negative charges on the oxygen atom in position 1. But because of resonance stabilization in **3** and **4**, the charge on the oxygen atom is slightly decreased. The slightly shorter CO bond lengths in these molecules also reflect the larger resonance contribution. These observations can be summarized as follows: All the molecules have large charge separation in the ground state, but in the case of **1**, **2**, and **5**, the diradicaloid form also contributes to a reasonable extent. In fact, the mixing coefficients of the doubly excited operator (HOMO−LUMO) in molecules **3** and **4** are much smaller (around 0.06) than in the other molecules (around 0.09) (Table 3). The dipole moment of the ground state indicates that **2** has a larger zwitterionic character when compared to **1**, due to charge stabilization.

Transition dipole moments along with the oscillator strengths and the transition energies obtained by SAC/SAC−CI for both B3LYP- and HF-based geometries are shown in Table 5. Energy of transition is lower in the molecules with more diradicaloid character. Thus, the lowest energy of transition is in **5**, and the highest is in **4**. It is clear from the transition dipole moment that the direction of the charge transfer is dominantly on one axis and it is perpendicular to the dipole moment and lies on the backbone of the molecule. The moments are reasonably large: In **2**, it is 13.32 D, while in **1**, it is smaller, 12.28 D. As this is a measure of charge transfer (CT), it indicates that charge transfer does take place. It is observed that the oscillator strength is smaller in **1** than in **2** (almost double). It is larger in **3** than in **1** and **2**, although the transition moment is not very different. This can be explained as follows: The oscillator strength is a function of not only the transition dipole moment but also the transition energy (product of ΔE and square of the transition dipole moment). The energy gap of **1** is the lowest of the three

molecules, which is reflected in the smaller oscillator strength. In **5**, the transition moment is smaller than in **1** or **2**, and the energy gap is much smaller; hence, it has the lowest oscillator strength. On this basis, we observe that, although **3** has almost equal CT to **2**, but the diradicaloid character is greater in **2**, the energy gap is smaller. This also indicates that the absorption shifting to the red will have a weaker intensity. The transition energies obtained for **1**, **2**, and **4** are in good agreement with the experimentally determined values.

C. Qualitative Molecular Orbital Picture. The MO energies of the five molecules are shown in Figure 3. It is clearly seen in **1**, **2**, and **5** that the HOMO-1 and HOMO-2 are nearly degenerate. The double excitation configurations from these orbitals contribute to the ground state as seen in Table 3. The paired double excitation from the HOMO−LUMO is the other low excitation and with a decreasing HOMO−LUMO gap plays a significant role. These create a diradical contribution with the electrons localized on the side rings. It should be noted that in the extreme case of entirely diradical character the HOMO and the LUMO would be degenerate. The conceptually simpler conventional CI wave function of the ground state and the wave function of the excited state in their respective symmetries are shown in terms of excitations between the orbitals.

$$^1A = c_1[HF] + c_2\langle a^{occ} \rightarrow a\rangle + c_3\langle b^{occ} \rightarrow b\rangle +$$
$$c_4\{\langle a^{occ} \rightarrow b\rangle + \langle a^{occ} \rightarrow b\rangle\} + c_5\{\langle b^{occ} \rightarrow a\rangle +$$
$$\langle b^{occ} \rightarrow a\rangle\} + c_6\{\langle a^{occ} \rightarrow a\rangle + \langle a^{occ} \rightarrow a\rangle\} +$$
$$c_7\{\langle b^{occ} \rightarrow b\rangle + \langle b^{occ} \rightarrow b\rangle\} + c_8\{\langle a^{occ} \rightarrow b\rangle + \langle b^{occ} \rightarrow a\rangle\}$$

$$^1B = d_1\langle b^{occ} \rightarrow a\rangle + d_2\langle a^{occ} \rightarrow b\rangle + d_3\{\langle a^{occ} \rightarrow b\rangle +$$
$$\langle a^{occ} \rightarrow a\rangle\} + d_4\{\langle a^{occ} \rightarrow b\rangle + \langle b^{occ} \rightarrow b\rangle\} +$$
$$d_5\{\langle b^{occ} \rightarrow a\rangle + \langle a^{occ} \rightarrow a\rangle\} + d_6\{\langle b^{occ} \rightarrow a\rangle + \langle b^{occ} \rightarrow b\rangle\}$$

It should be stressed that the c_1 and d_1 coefficients in both cases are the largest, while the others have smaller coefficients, such as in the case of the double excitation, but these in no way can be neglected here. The double excitation contributions start increasing if the gap between the orbitals is brought down either by substitution or changes in geometry like rotation. Working out the one-electron matrix elements for the transition dipole moment integral $\langle ^1A|R|^1B\rangle$, it is seen that the only surviving elements are the single excitations, as expected.

$$c_1'\langle b \rightarrow a\rangle + c_2'\langle b \rightarrow a\rangle + c_3'\langle a \rightarrow b\rangle + c_4'\langle a \rightarrow b\rangle$$

Where the single excitations in the integral like $\langle a \rightarrow b + a \rightarrow b|r|a \rightarrow b\rangle$ have projected out the single excitations from

TABLE 5: Excitation Energy ΔE, Oscillator Strength f, and Transition Dipole Moments of All Structures Calculated Using SAC−CI for the B3LYP/6-31G(d,p) and HF/6-31G(d,p)[a] Optimized Geometries[b]

molecule	ΔE^c (eV)	f	experimental (eV)	transition	transition dipole moment (debye)		
					X	Y	Z
1	1.043	0.596	1.127[d]	$^1A \rightarrow {}^1B$	0.13	12.28	0.00
	(1.111)	(0.612)			(0.06)	(12.06)	(0.00)
2	1.500	1.008	1.409[d]	$^1A \rightarrow {}^1B$	0.25	13.32	0.00
	(1.537)	(0.977)			(0.32)	(12.94)	(0.00)
3	1.720	1.156	-	$^1A \rightarrow {}^1B$	0.03	13.32	0.00
	(1.760)	(1.147)			(0.09)	(13.11)	(0.00)
4	2.971	0.385	2.818[e]	$^1A_1 \rightarrow {}^1B_2$	0.00	5.85	0.00
	(3.059)	(0.382)			(0.00)	(5.74)	(0.00)
5	1.000	0.390	-	$^1A \rightarrow {}^1B$	0.08	10.14	0.00
	(1.048)	(0.385)			(0.08)	(9.85)	(0.00)

[a] Values obtained at HF/ 6-31G (d, p) level are in parentheses. [b] Experimental excitation energies are also given for molecules **1**, **2**, and **4**. [c] ΔE = vertical excitation energy from the ground to the first excited state. [d] Ref 6. [e] Ref 2.
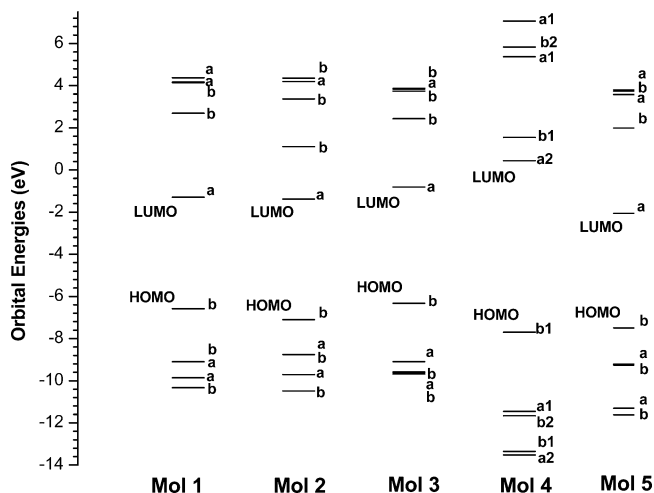
Figure 3. Molecular orbital energy levels (five highest occupied and five lowest unoccupied) of molecules **1**–**5**.
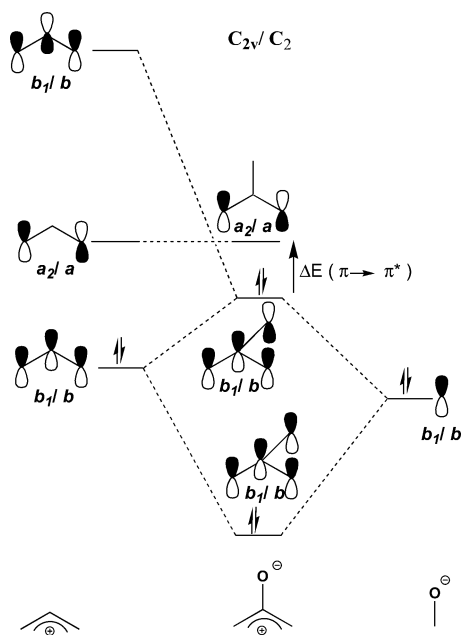

Figure 4. Orbital interaction diagram for allyl cation and oxygen anion.

the paired double excitations. Here, c_2' and c_4' have smaller contributions, as they are projected out of the double excitations.

We now draw the qualitative MO picture of the oxyallyl substructure. On the basis of our ab initio calculations reported in earlier sections, we propose that the zwitterionic structure shown in Figure 1d, which is indicative of an allyl cation interacting with an oxygen anion, will represent the substructure present in the larger molecule. Such an MO diagram for C_{2v}/C_2 is shown in Figure 4, where the three MOs of the cation, namely, the fully symmetric and filled MO b_1/b, the lower-lying a_2/a orbital which is now empty because of the positive charge, and the higher-lying antibonding b_1/b orbital, interact with the O p_z orbital which is completely filled because of the negative charge. Because of symmetry, the b_1/b MOs of the allyl cations have an in-phase and out-of-phase mixing with the oxygen p_z orbital. This creates a lower-energy MO with a b_1/b symmetry, while its out-of-phase combination becomes the HOMO in this case with two electrons filled. The a_2/a orbital of the allyl cation does not mix with the oxygen and remains unaffected, and still lies higher in energy. This is now the LUMO. From this simple picture, it can be seen that the HOMO–LUMO gap is highly reduced, and the one-electron transition is π–π^* with some charge transfer from the oxygen atom in the excited state. Bigelow and Freund observed in their work that the charge transfer from the oxygen atom to the moiety in the excited state increases the transition energy in the squaraine-based dyes.[16] The effect of the orbital interactions, due to the neighboring groups and the changes in geometry of the substructure in the molecule, either stabilizes or destabilizes the MOs and plays a crucial role. These are shown in Figure 5. These shifts are will be analyzed on the basis of the structure and substitutions.

The effect of substituting NH$_2$ in the 3 and 4 positions on the HOMO–LUMO gap is shown in Figure 5 along with the unsubstituted croconic acid (R = H in Figure 1b) for comparison. These orbital energies have been obtained at the HF/6-31G(d,p) level. The amino groups stabilize the HOMO, and in the LUMO, because of the antibonding interaction, a destabilization occurs. On the other hand, all the occupied orbitals experience stabilization due to the interaction with the p$_z$ orbital of the substituent groups, and all the unoccupied orbitals destabilize and in effect create a larger gap between the bonding and antibonding orbitals. With the larger gap between the frontier orbitals, the transition dipole moment also decreases. Such a case is seen in molecule **4**. On the other hand, if the conjugation is increased, although the HOMO–LUMO gaps start becoming smaller, the transition energy is larger, as in **3**.
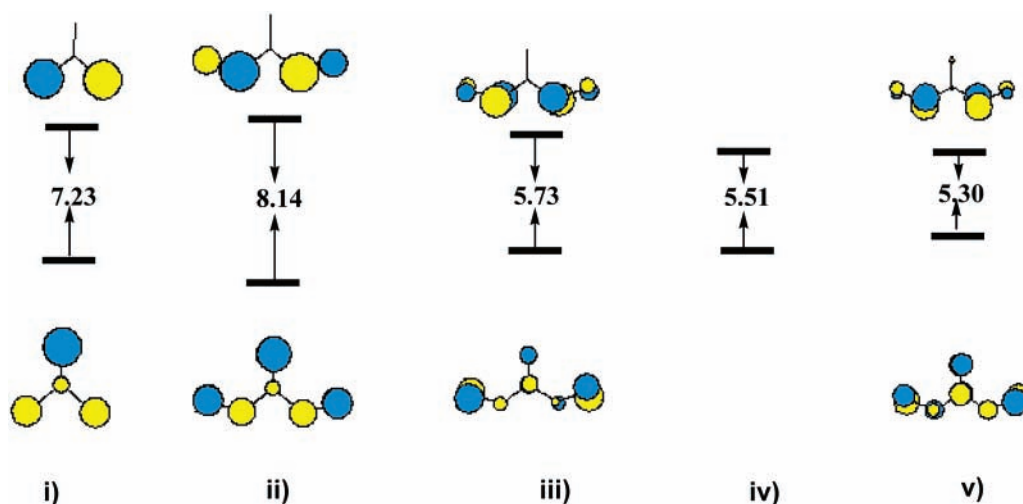

Figure 5. HOMO–LUMO gaps (eV) for (i) oxyallyl substructure in unsubstituted croconic acid (R = H in Figure 1b), (ii) molecule **4**, (iii) molecule **2**, (iv) molecule **3**, and (v) molecule **1**.

Oxyallyl-Substructure-Based NIR Dyes

J. Phys. Chem. A, Vol. 109, No. 11, 2005 **2621**

For these planar conjugated molecules, the effect of the donor groups could play a major role. Rotating the side groups to break the conjugation increases the HOMO−LUMO gap slightly, but the break in symmetry brings about degeneracy in some lower occupied orbitals. Hence, lower transition energy is obtained, as in **2**.

We now see the effect of twisting the orbitals of the substructure, due to substitutions which are either bulky or which rotate out of the plane to prevent the steric interactions. Such is the case for **1** where the twist angle is around 27° compared to 4° in **2** (angle 5324 of Figure 1). Here, it is seen that the HOMO, which has a bonding interaction between the p_z orbitals of the 3,4-positions due to the rotation, has an increase of the antibonding interaction, or in other words, the HOMO is destabilized by the rotation. On the other hand, the LUMO, because of the rotation, has now increased bonding interactions which stabilize the LUMO further. In other words, this means that because of the rotation the HOMO−LUMO gap decreases as shown in the figure. The effect of rotation is that all the occupied orbitals *b* now also experience a destabilization, and all the unoccupied *a* orbitals experience a stabilization, with the net effect that the orbital gaps between the unoccupied *a* and the occupied *b* decrease.

Large positive-charge delocalization on the backbone and negative charge on the oxygen atom favors a zwitterionic structure and intense absorption (HOMO−LUMO excitation is dominating). Reduction of this positive charge on the backbone, either by geometry or electronic changes, creates a more diradicaloid character (greater role for double excited CI). Because of the smaller energy differences between the orbitals, a larger interaction takes place, and a red shift can be observed but with less intensity. The role of the donor in the red shift is now clearer in **5** (Table 5) where the amino groups have been removed. The excitation energy is nearly the same as in **1** (red-shifted by 70 nm), but the oscillator strength, *f*, is decreased. This decrease in *f* is also indicative of less stabilization of the positive charge on the backbone of the molecule in the absence of the amino groups. Further proof is the smaller dipole moment of 2.25 D when compared to 2.37 D in **1**. In the case of **2** and **3**, it is seen that although **3** has a smaller HOMO−LUMO gap the absorption spectra is red-shifted in **2**. This is because the conjugation helps to stabilize the positive charge in **3** and creates a zwitterionic kind of structure (seen with larger dipole moment in Table 2), while distortion in **2** brings the orbitals closer to each other. Thus, *f* is smaller in **2** than in **3** because of the larger contributions from the diradicaloids at the CI level, due to the twisted orbital interactions.

Conclusions

Because the oxyallyl substructure is a diradicaloid derivative, it is important that other than the singles CI the doubles CI has to be included to describe the ground and excited states and to study the excitations in its dyes. The energies of these (HOMO−LUMO gap) in general lie in the red region, so even a small energy contribution from a singly or doubly excited configuration will show up as a reasonably large shift in the spectrum. As the molecular orbitals lie close to each other, a small orbital energy change also shows up as a large shift in the absorption via the CI. Thus, these chromophore-based derivatives such as the croconium dyes show a large shift in the spectra with small geometrical changes. When the symmetry of the substructure is reduced from C_{2v} to C_2 by twisting, stronger interactions at the orbital level are seen. This produces a large bathochromic shift which is observed in the BM dye (Figure 1c). The role of the donors in the red shift is small, while the carbonyl groups and the hydroxyl groups stabilize the charge separation, rather than act as withdrawing/donating groups. The amino groups and the large conjugation help to stabilize the positive charge in the ground state.

References and Notes

(1) Fabian, J. *Chem. Rev.* **1992**, *92*, 1197.

(2) Fabian, J.; Zahradnik, R. *Angew. Chem., Int. Ed. Eng.* **1989**, *28*, 677.

(3) Law, K. Y. *Chem. Rev.* **1993**, *93*, 449.

(4) (a) *IR Absorbing Dyes*; Matsuoka, M., Ed.; Plenum Press: New York, 1990. (b) *Near-Infrared Dyes for High Technology Applications*; Daehne, S., Resch-Genger, U., Wolfbeis, O. S., Eds.; NATO ASI Series 3; Kluwer Academic: Dordrecht, The Netherlands, 1998; Vol. 52.

(5) Tian, M.; Tatsuura, S.; Furuki, M.; Sato, Y.; Iwasa, I.; Pu, L. S. *J. Am. Chem. Soc.* **2003**, *125*, 348.

(6) Tatsuura, S.; Tian, M.; Furuki, M.; Sato, Y.; Iwasa, I.; Mitsu, H. *Appl. Phys. Lett.* **2004**, *84*, 1450.

(7) Tatsuura, S.; Mastubara, T.; Tian, M.; Mitsu, H.; Iwasa, I.; Sato, Y.; Furuki, M. *Appl. Phys. Lett.* **2004**, *85*(4), 540.

(8) Langhals, H. *Angew. Chem., Int. Ed. Eng.* **2003**, *42*, 4286.

(9) KÖnig, W. *J. Prakt. Chem.* **1925**, *112*, 1.

(10) Ismailsky, W. Dissertation, Universität Dresden, 1913.

(11) Dilthey, W.; Wizinger, R. *J. Prakt. Chem.* **1928**, *118*, 321.

(12) Wizinger, R. *Chimia* **1961**, *15*, 89.

(13) Griffiths, J. *Colour and Constitution of Organic Molecules*; Academic Press: London, 1976.

(14) Dähne, S.; Kulpe, S. *Structural Principles of Unsaturated Organic Compounds*; Akademic Verlag: Berlin, 1977 (*Abh. Akad. Wiss. DDR 8*).

(15) Dewar, M. J. S.; Dougherty, R. C. *The PMO Theory of Organic Chemistry*, 1st ed.; Plenum: New York, 1975; pp 410−418.

(16) Bigelow, R. W.; Freund, H. J. *Chem. Phys.* **1986**, *107*, 159.

(17) Meyers, F.; Chen, C. T.; Marder, S. R.; Bredas, J. L. *Chem.−Eur. J.* **1997**, *3*, 530.

(18) Yang. M.; Jiang, Y. *Phys. Chem. Chem. Phys.* **2001**, *3*, 4213.

(19) Dirac, C. W.; Herndon, W. C.; Cervantes-Lee, F.; Selnau, H.; Martinez, S.; Kalamegham, P.; Tan, A.; Campos, G.; Velez, M.; Zyss, J.; Ledoux, I.; Cheng, L. T. *J. Am. Chem. Soc.* **1995**, *117*, 2214.

(20) Law, K. Y. *J. Phys. Chem.* **1987**, *91*, 5184.

(21) Meier, H.; Petermann, R.; Gerold, J. *Chem. Commun.* **1999**, 977.

(22) (a) Seitz, G.; Auch, J.; Klein, W. *Chem.-Ztg.* **1987**, *87*, 343. (b) Nishimura, Y.; Kimura, T.; Matsuda, H.; Eguchi, T.; Nakagiri, T.; Sakai, K. Jpn. Kokai Tokkyo Koho 62149482; *Chem. Abstr.* **1988**, *109*, 214047t.

(23) Bariller, D. *Phosphorous Sulfur Relat. Elem.* **1980**, *8*, 79.

(24) Nakajima, T.; Nakatsuji, H. *Chem. Phys. Lett.* **1997**, *280*, 79.

(25) Wan, Jian.; Ehara, M.; Hada, M.; Nakatsuji, H. *J. Chem. Phys.* **2000**, *113*, 5245.

(26) Nakajima, T.; Nakatsuji, H. *Chem. Phys. Lett.* **1999**, *300*, 1.

(27) Wan, J.; Hada, M.; Ehara, M.; Nakatsuji, M. *J. Chem. Phys.* **2001**, *114*(2), 842.

(28) (a) Nakatsuji, H. *Acta Chim. Hung.* **1992**, *129*, 719. (b) Nakatsuji, H. In *Computational Chemistry−Reviews of Current Trends*; Leszczynski, J., Ed.; World Scientific: River Edge, NJ, 1997; Vol. 2.

(29) Gleiter, R.; Hoffmann, R. *Angew. Chem.* **1969**, *81*, 225.

(30) Hrovat, D. A.; Murcko, M. A.; Lahti, P. M.; Borden, W. T. *J. Chem. Soc., Perkin Trans.* **1998**, *2*, 1037.

(31) Kole, J.; Michl, J. *J. Am. Chem. Soc.* **1973**, *95*, 7391.

(32) (a) Foresman, J. B.; Head-Gordon, M.; Pople, J. A.; Frish, M. J. *J. Phys. Chem.* **1992**, *96*, 135. (b) Head-Gordon, M.; Rico, R. J.; Oumi, M.; Lee, T. J. *Chem. Phys. Lett.* **1994**, *219*, 21.

(33) (a) Bacon, A. D.; Zerner, M. C. *Theo. Chim. Acta* **1979**, *53*, 21. (b) Anderson, W. P.; Edwards, W. D.; Zerner, M. C. *Inorg. Chem.* **1986**, *25*, 2728.

(34) Frisch, M. J.; Trucks, G. W.; Schlegel, H. B.; Scuseria, G. E.; Robb, M. A.; Cheeseman, J. R.; Montgomery, J. A., Jr.; Vreven, T.; Kudin, K. N.; Burant, J. C.; Millam, J. M.; Iyengar, S. S.; Tomasi, J.; Barone, V.; Mennucci, B.; Cossi, M.; Scalmani, G.; Rega, N.; Petersson, G. A.; Nakatsuji, H.; Hada, M.; Ehara, M.; Toyota, K.; Fukuda, R.; Hasegawa, J.; Ishida, M.; Nakajima, T.; Honda, Y.; Kitao, O.; Nakai, H.; Klene, M.; Li, X.; Knox, J. E.; Hratchian, H. P.; Cross, J. B.; Adamo, C.; Jaramillo, J.; Gomperts, R.; Stratmann, R. E.; Yazyev, O.; Austin, A. J.; Cammi, R.; Pomelli, C.; Ochterski, J. W.; Ayala, P. Y.; Morokuma, K.; Voth, G. A.; Salvador, P.; Dannenberg, J. J.; Zakrzewski, V. G.; Dapprich, S.; Daniels,

A. D.; Strain, M. C.; Farkas, O.; Malick, D. K.; Rabuck, A. D.; Raghavachari, K.; Foresman, J. B.; Ortiz, J. V.; Cui, Q.; Baboul, A. G.; Clifford, S.; Cioslowski, J.; Stefanov, B. B.; Liu, G.; Liashenko, A.; Piskorz, P.; Komaromi, I.; Martin, R. L.; Fox, D. J.; Keith, T.; Al-Laham, M. A.; Peng, C. Y.; Nanayakkara, A.; Challacombe, M.; Gill, P. M. W.; Johnson,

B.; Chen, W.; Wong, M. W.; Gonzalez, C.; Pople, J. A. *Gaussian 03*, revision B.01; Gaussian, Inc.: Pittsburgh, PA, 2003.

(35) Hu, Z.; Boyd, R. J.; Nakatsuji, H. *J. Am. Chem. Soc.* **2002**, *124*, 2664.

(36) Lichtenberger, D. L.; Fenske, R. F. *QCPE* **1975**, *11*, 284.